SLAC-PUB-13835

A Multi-Wavelength Investigation of the Unidentified Gamma-Ray Source HESS J1708-410

Adam Van Etten[1], Stefan Funk[1], & Jim Hinton[2]

ave@stanford.edu, sfunk@stanford.edu, j.a.hinton@leeds.ac.uk

ABSTRACT

We report on recent XMM-Newton observations, archival radio continuum and CO data, and SED modeling of the unidentified Galactic plane source HESS J1708-410. No significant extended X-ray emission is observed, and we place an upper limit of $3.2 \times 10^{-13}\,\mathrm{erg\,cm^{-2}\,s^{-1}}$ in the 2-4 keV range for the region of TeV emission. Molonglo Galactic Plane Survey data is used to place an upper limit of 0.27 Jy at 843 MHz for the source, with a 2.4 GHz limit of 0.4 Jy from the Parkes survey of the southern Galactic plane. ^{12}CO (J 1→0) data of this region indicates a plausible distance of 3 kpc for HESS J1708-410. SED modeling of both the H.E.S.S. detection and flux upper limits offer useful constraints on the emission mechanisms, magnetic field, injection spectrum, and ambient medium surrounding this source.

Subject headings: gamma rays: observations — X-rays: general — radiation mechanisms: non-thermal

1. Introduction

Since beginning operation in 2004 the H.E.S.S. Cherenkov telescope array has proven a valuable tool in the investigation of extremely energetic phenomena, yielding ~ 50 very-high-energy (VHE) Galactic gamma-ray sources. Roughly half of these sources lack definitive counterparts at longer wavelengths, and a few lack *any* plausible counterpart. The firmly identified Galactic TeV sources consist of Supernova remnants (SNRs), Pulsar Wind Nebulae (PWNe) and high-mass X-ray binaries (HMXBs). There are also plausible associations with young and massive stellar clusters (Aharonian et al. 2007), and dense molecular clouds

[1]Department of Physics, Stanford University, Stanford, CA 94305

[2]School of Physics & Astronomy, University of Leeds, Leeds LS2 9JT, UK

KIPAC, SLAC National Accelerator Center, 2575 Sand Hill Road, Menlo Park, CA 94309
Work supported in part by US Department of Energy contract DE-AC02-76SF00515.

(Aharonian et al. 2006a). Those TeV sources with no low energy counterpart may be underluminous (at longer wavelengths) members of these source classes, or may represent an entirely new class of TeV source. Understanding these so called 'dark accelerators' with no identified counterpart at other wavebands is one of the more intriguing challenges of high energy astrophysics.

Gamma-rays in the VHE regime invariably arise from nonthermal particle populations, though for a given source determining if this population is dominantly leptonic or hadronic often proves quite challenging. For leptons in low density environments, inverse-Compton (IC) upscattering of background photons off highly relativistic electrons dominates, while bremsstrahlung becomes important only amongst very dense surroundings. For any scenario in which the gamma-ray emission arises from relativistic electrons, significant X-ray synchrotron emission can be expected, with a peak synchrotron flux comparable to the peak IC flux for typical galactic magnetic field strengths and radiation densities. This synchrotron emission usually extends down to radio energies with emission from lower energy, $\mathcal{O}(1$ GeV), electrons. Yet if the electron spectrum within a source is truncated at low energies a bright TeV source may be unaccompanied by a radio counterpart. Such a situation is plausible for PWNe, given that the lowest particle energy is determined primarily by the four velocity of the pulsar wind upstream of the termination shock (Kennel & Coroniti 1984) which is in turn linked to observable shock properties such as synchrotron luminosity and shock radius. A hard electron spectrum with index greater than the canonical value of -2 might also result in an underluminous radio counterpart given the relative lack of low energy electrons. Hadronic acceleration results in the production of neutral pions via proton-proton interactions, which decay to produce VHE gamma rays. Proton interactions also produce charged pions and hence secondary electrons that in turn produce synchrotron radiation in the radio to X-ray range, albeit usually at a much lower level than in leptonic scenarios. Nevertheless, in both scenarios, at least a weak lower energy counterpart is expected. Probing this lower energy regime provides insights into the particle population, ambient medium properties, and magnetic field strength.

HESS J1708−410 (hereafter J1708) is one of the relatively few VHE gamma-ray sources for which *no* plausible explanation has yet been put forward. It was discovered during the H.E.S.S. survey of the inner Galaxy, as described by (Aharonian et al. 2006c). Subsequent observations improved the statistical significance to 11σ over a total livetime of 39 hours (Aharonian et al. 2008). J1708 is only slightly extended with respect to the H.E.S.S. point spread function, consistent with a marginally elongated Gaussian of approximately $0.06^\circ \times 0.08^\circ$. Aharonian et al. (2008) report no significant emission beyond 0.3°, ruling out an association with the nearby SNR G 345.7−0.2. The nearest known pulsar (PSR J1707–4053) lies exterior to our XMM field of view $\sim 15'$ northwest of the H.E.S.S. centroid, and is

several orders of magnitude too weak ($\dot{E} \sim 4 \times 10^{32}\,\mathrm{erg\,s^{-1}}$) and too old ($\tau_c \sim 5 \times 10^6$ years) to conceivably power the TeV emission. Aharonian et al. (2008) fit the H.E.S.S. source spectrum over the energy range of 0.50–60 TeV and an aperture of 0.3° to fully enclose the source. This yields a power-law index of −2.5 and a flux of $\approx 8{\times}10^{-12}\,\mathrm{erg\,cm^{-2}\,s^{-1}}$. An archival ASCA pointing of this region shows only a single point source located over a degree from the H.E.S.S. source. In addition, a previous XMM-Newton exposure of G 345.7−0.2 revealed no X-ray emission at the H.E.S.S. position, though this pointing placed J1708 close to the edge of the field of view. In this paper we report on new XMM-Newton observations of this enigmatic VHE source.

2. Observations and Data Analysis

J1708 was observed with the European Photon Imaging Cameras (EPIC) aboard the XMM-Newton satellite in imaging mode with the medium filter on 2006-08-25 through 2006-08-26. The calibration, data reduction, and analysis rely upon the XMM-Newton Science Analysis Software (SAS [1]) version 8.0.0. Following the standard procedure, the data were filtered to reduce background caused by soft proton flares. As such flaring was minimal in this observation, 24.0 ks of the total of 26.7 ks remain after filtering for both the MOS1 and MOS2 camera. For the PN camera the 27.0 ks were whittled down to 21.6 ks. The MOS cameras, with fewer chip gaps than the PN camera, are better suited to imaging. Figure 1 shows a mosaic of the MOS1 and MOS2 detectors revealing no sign of diffuse emission save for hard (> 2 keV) reflection contamination from an unknown bright source outside the field of view.

2.1. Counterparts Search

Within the XMM-Newton field of view a number of point sources are detected. No obvious extended emission is seen with the exception of contaminating reflections from a nearby bright X-ray source at energies above 2 keV (see Figure 1). Two ROSAT hard-band X-ray sources exist to the northeast: 0.3° away lies J171011.5-405356, and slightly farther away is LMXB 4U 1708-40, either of which could be responsible for the reflection patterns.

We employ the SAS function edetect_chain for source detection and search in two energy

[1]The XMM-Newton SAS is developed and maintained by the Science Operations Centre at the European Space Astronomy Centre and the Survey Science Centre at the University of Leicester.

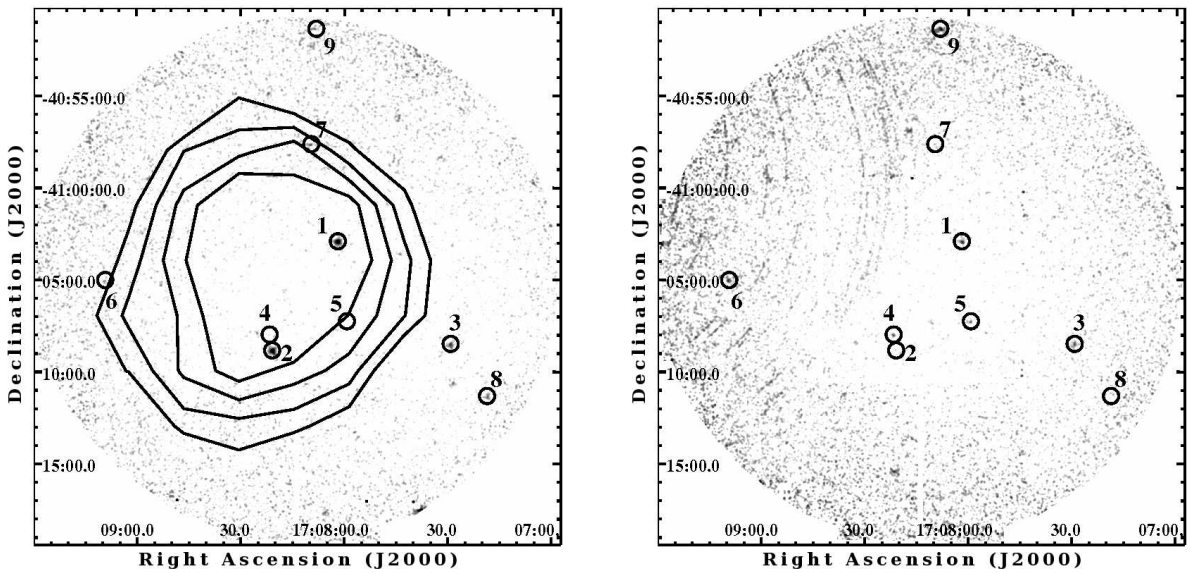

Fig. 1.— Left: EPIC MOS exposure corrected $0.3-2$ keV image with $5.5''$ Gaussian smoothing. The H.E.S.S. 5, 6, 7, and 8 σ contours are overlaid, and point sources indicated. Right: EPIC MOS exposure corrected $2-10$ keV image with $5.5''$ Gaussian smoothing exhibiting the reflection contamination. Neither image indicates any sign of extended emission (save for contamination).

bands of $0.3-2$ keV and $2-10$ keV for sources with a probability $P < 10^{-13}$ of arising from random Poissonian fluctuations. This rigorous cutoff threshold is necessary due to the aforementioned contaminating streaks. 10 sources are detected, although we remove 1 source which lies directly along the arcs of reflection and has 0 counts in the soft band. The source detection algorithm also attempts to determine source extension via a Gaussian model, though all detections are consistent with a point source. Table 1 lists the X-ray data. We define the hardness ratio as: HR=$(C_{hi}-C_{lo})/(C_{hi}+C_{lo})$ where C_{lo} and C_{hi} are MOS counts in the $0.3-2$ keV and $2-10$ keV bands, respectively. The only source with a cataloged SIMBAD counterpart is source 2, which coincides with field star HD 326944 of magnitude ~ 10 and type G0. Sources 1 and 3 lie within $1''$ of USNO-B1.0 12th and 18th magnitude sources, respectively. Only sources 1 and 2 have sufficient counts to extract meaningful point source spectra, though fits to these sources are still accompanied by large errors. Source 1 is best matched with an absorbed power law, with hydrogen column density hardly constrained at $n_H = 2.0^{+2.7}_{-2.0} \times 10^{21}\,\mathrm{cm}^{-2}$ (90% single parameter errors). As such we fix n_H at $2.0 \times 10^{21}\,\mathrm{cm}^{-2}$ and measure an index of $2.9^{+0.5}_{-0.4}$ and unabsorbed 0.3–10 keV flux of $1.3 \pm 0.3 \times 10^{-13}\,\mathrm{erg\,cm^{-2}\,s^{-1}}$. Source 2 (HD 326944) is best modeled by an absorbed mekal plasma, with n_H again essentially unconstrained at $1.3^{+5.4\times10^5}_{-0.6} \times 10^{16}\,\mathrm{cm}^{-2}$. With n_H fixed

at $1.0 \times 10^{16}\,\mathrm{cm}^{-2}$ we find a temperature of $kT = 0.49^{+0.09}_{-0.10}\,\mathrm{keV}$ and unabsorbed 0.3–10 keV flux $4.2^{+0.5}_{-0.7} \times 10^{-14}\,\mathrm{erg\,cm^{-2}\,s^{-1}}$.

The 73 ms time resolution of the PN camera allows searches for periodicities from a possible pulsar candidate to be conducted; the MOS datasets have a time resolution of 2.6 s, insufficient to search for a signal from a typical rotation powered pulsar. To this end, for each of the three brightest point sources we barycenter the events, extract a lightcurve, and search for periodicities within the PN dataset with the *Xronos* function *powspec*; no significant periodicities are detected.

Table 1: Source Properties

No.	R.A.	Dec.	Pos. Err.($''$)	Counts	HR
1	17 : 08 : 01.81	−41 : 02 : 55.2	0.37	784.1 ± 33.4	-0.65 ± 0.035
2	17 : 08 : 20.81	−41 : 08 : 51.2	0.32	624.4 ± 29.5	-0.97 ± 0.020
3	17 : 07 : 29.29	−41 : 08 : 29.4	0.46	186.8 ± 17.6	-0.26 ± 0.096
4	17 : 08 : 21.68	−41 : 07 : 59.5	0.73	72.7 ± 12.1	$+0.73 \pm 0.14$
5	17 : 07 : 59.38	−41 : 07 : 16.0	1.07	57.0 ± 11.1	$+0.82 \pm 0.15$
6	17 : 09 : 09.23	−41 : 05 : 00.8	1.43	59.1 ± 11.1	$+0.47 \pm 0.16$
7	17 : 08 : 09.66	−40 : 57 : 38.4	1.15	60.2 ± 11.2	-0.79 ± 0.17
8	17 : 07 : 18.60	−41 : 11 : 18.9	1.46	56.8 ± 10.8	-0.85 ± 0.18
9	17 : 08 : 08.13	−40 : 51 : 22.2	0.93	88.7 ± 14.2	$+0.57 \pm 0.13$

We analyzed ^{12}CO (J 1→0) data from the survey of Dame et al. (2001) to search for molecular cloud associations with J1708, constrain the target material density, and estimate the distance to J1708. Figure 2 shows the CO velocity profile along the line of sight to J1708 in the single $0.15^\circ \times 0.15^\circ$ pixel which covers the TeV source. A single major molecular complex is visible in this profile with a probable distance of $\approx 3 \pm 1$ kpc, adopting the Galactic rotation curve of (Brand & Blitz 1993) and assuming a near solution. Effectively all massive star formation occurs in molecular clouds, and all known Galactic TeV sources are related to massive stars or their end products (PWN, SNR, etc.). As such, this 3 ± 1 kpc distance (corresponding to the near side of the Molecular Ring of the Milky Way) seems the most likely location for HESS J1708−410. We therefore assume a distance of 3 kpc in all subsequent discussions and scale distances by $d_3 \equiv d/(3\,\mathrm{kpc})$. A more speculative alternative possibility is that J1708 is associated with the $\sim 0.1^\circ$ cavity suggested by the Spitzer image of Figure 3, and comparable in size to the H.E.S.S. source. The region of low infrared emission towards the center of J1708 also seems to correspond to a hole in the nearby ($\sim$1 kpc) CO emission. We could perhaps be looking at a bubble blown by an SNR or stellar wind. There is, however, no evidence of a stellar cluster at the center of this bubble, which undermines this hypothesis.

An upper limit on the density inside the source can be derived from the column density towards the source and the observed source size ($\theta = 10'$ FWHM) $n \leq n_H/\theta\, D$. For the measured molecular column around 3 kpc of $\approx 5 \times 10^{21}\,\mathrm{cm}^{-2}$ (24 K km with a conversion

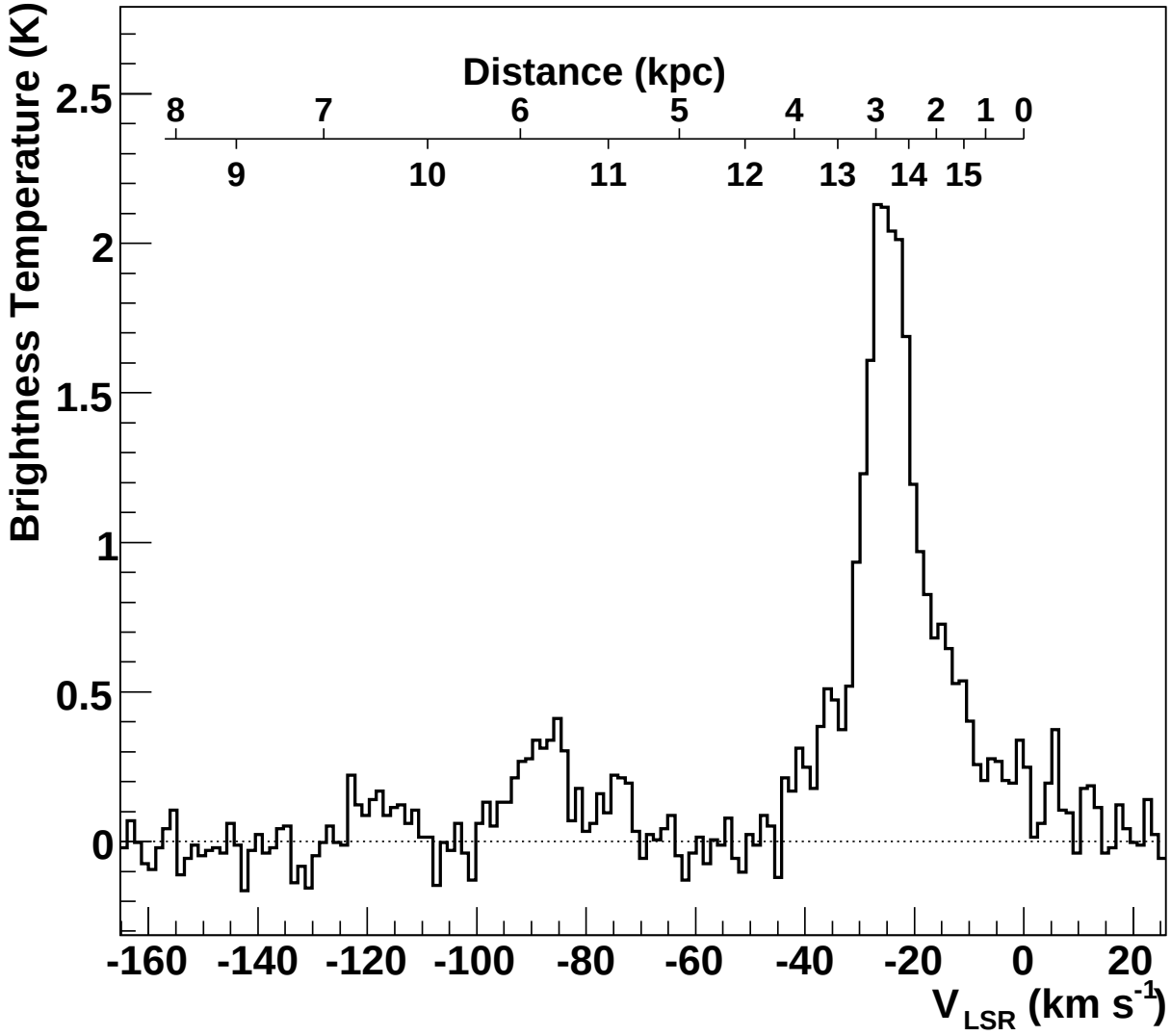

Fig. 2.— CO velocity profile in the vicinity of J1708 showing the single major molecular complex along the line of sight, with a probable distance of 3 kpc. The correspondence of velocity to distance (from the galactic rotation curve of Brand & Blitz 1993) is inset.

factor $X \approx 2 \times 10^{20}\,\mathrm{cm}^{-2}$ / (K km)) this corresponds to $n \leq 200\,d_3^{-1}\,\mathrm{cm}^{-3}$. Note that the dominance of bremsstrahlung over IC on the CMBR at photon energies of 1 TeV requires $n > 240\,\mathrm{cm}^{-3}$ for an E^{-2} electron spectrum (Hinton & Hofmann 2009). We therefore neglect bremsstrahlung as an emission mechanism in the discussions below.

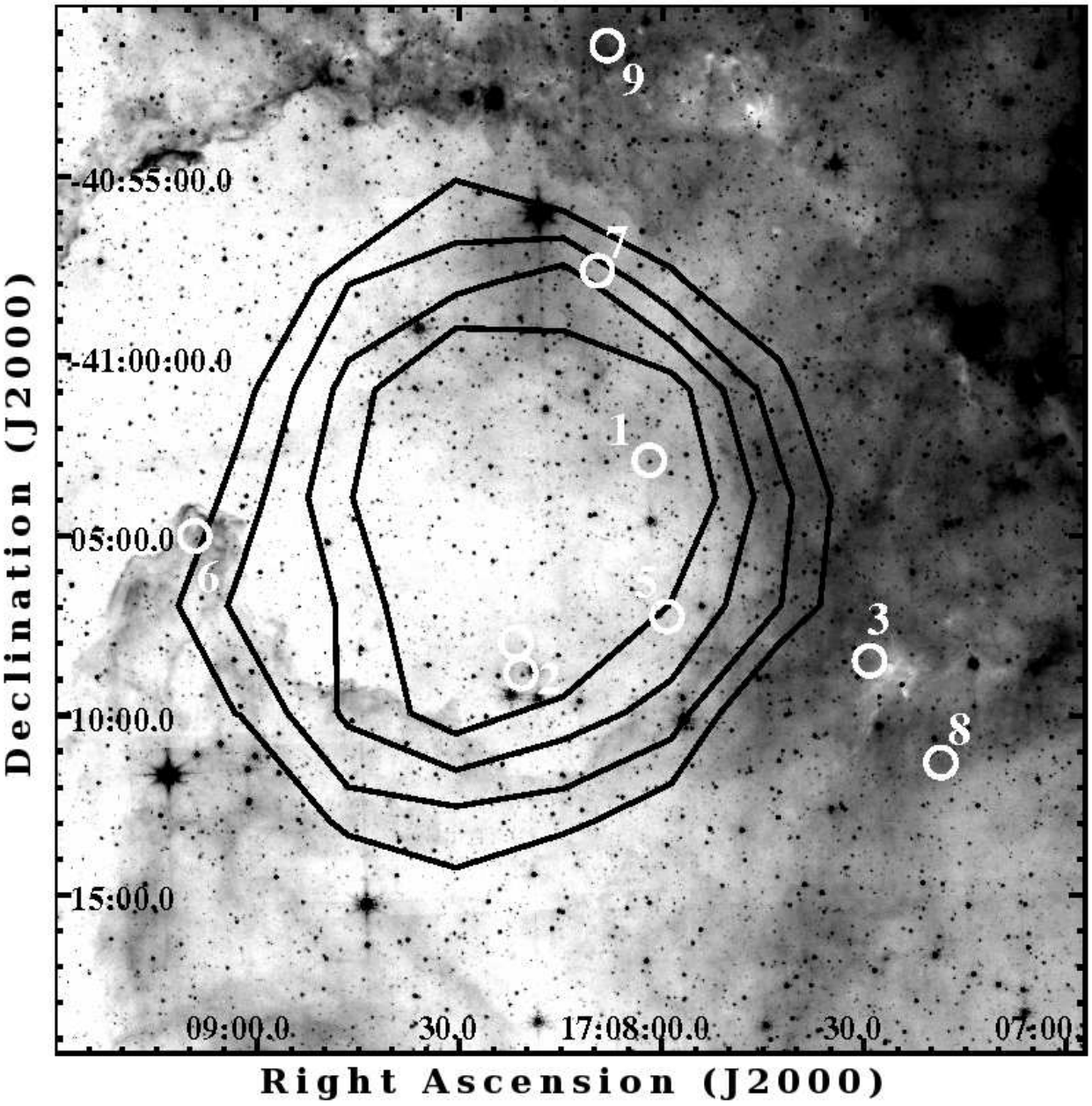

Fig. 3.— GLIMPSE Spitzer 8 μm image of the field of view of the XMM exposure, showing an apparent cavity coincident with J1708. H.E.S.S. significance contours and XMM source positions are overlaid.

2.2. Extended Source Spectral Analysis

In the absence of any obvious extended X-ray emission from J1708, we fit the flux and use this as an upper limit. To calculate this upper limit we define a region free of X-ray

point sources and scattered light contamination within the innermost (8σ) H.E.S.S. contour. This region encompasses 18% of the flux from the H.E.S.S. spectral integration area. We extract the spectrum from this region with the SAS task evselect, and generate response files with the tasks arfgen and rmfgen. The background is taken from a region near the outer edge of the chip, exterior to the H.E.S.S. contours. Spectra from both the MOS1 and MOS2 chips are fitted to a simple absorbed power law. This fit yields a hydrogen column density of $2.1 \pm 1.2 \times 10^{21}\,\mathrm{cm}^{-2}$, which can be compared to calculations from HI maps of the total galactic column density. (Kalberla et al. 2005) estimate a column of $1.34{\times}10^{22}\,\mathrm{cm}^{-2}$, and (Dickey & Lockman 1990) tabulate $1.65{\times}10^{22}\,\mathrm{cm}^{-2}$. While one cannot make any strong statements with these estimates, it does at least indicate that the fit hydrogen column density is consistent with a Galactic origin.

Scaling up the unabsorbed power law flux by the flux ratio of 1/0.18 (i.e. assuming matching X-ray and TeV morphology) provides a 90% flux limit of $1.8 \times 10^{-12}\,\mathrm{erg\,cm^{-2}\,s^{-1}}$ in the 0.3–10 keV range, and a limit of $3.2 \times 10^{-13}\,\mathrm{erg\,cm^{-2}\,s^{-1}}$ between 2 and 4 keV. The 2–4 keV limit is far less sensitive to the estimated column density to the source, so we quote this value in the following discussion.

While no deep radio images are available in this locale, we can extract upper limits from two major surveys of the southern Galactic plane. The first epoch Molonglo Galactic Plane Survey is a radio continuum survey at 843 MHz with a beam of $43'' \times 65''$ at the source position, and root-mean-square sensitivity of $1 - 2\,\mathrm{mJy\,beam^{-1}}$ (Green et al. 1999). There is no sign of diffuse emission close to J1708 in the relevant Molonglo image; one point-like source exists within the H.E.S.S. contours, but does not coincide with any of the XMM sources. We calculate a conservative mean surface brightness of $3\,\mathrm{mJy\,beam^{-1}}$ within the source region, and integrate over the $0.06^\circ \times 0.08^\circ$ extent to derive a flux density upper limit of 270 mJy. Higher frequency radio upper limits are available from the Parkes 2.4 GHz survey of the southern Galactic plane; images have a resolution of $10.4'$ ($\approx$ the size of J1708) with rms noise of approximately $12\,\mathrm{mJy\,beam^{-1}}$ (Duncan et al. 1995). We see no indication of a source at the position of J1708, and derive an upper limit of $400\,\mathrm{mJy\,beam^{-1}}$. As the source size is approximately the same as the beam size, we place a flux density upper limit of 400 mJy at 2.4 GHz.

3. Emission Scenarios

The X-ray and radio flux limits place significant restrictions on possible γ-ray emission mechanisms for J1708, which we explore by modeling its spectral energy distribution (SED). In Figures 4 and 5 we plot the SED of J1708 for both leptonic and hadronic scenarios, showing

the observed upper limits along with the H.E.S.S. detection. Also indicated is the one year sensitivity of the Large Area Telescope aboard the Fermi Gamma-ray Space Telescope (Abdo et al. 2009). To test these scenarios we apply a single-zone time-dependent numerical model with constant injection luminosity. We inject a power law spectrum of relativistic particles (either electrons or protons) with a high energy exponential cutoff, and then evolve this spectrum over time according to radiation losses from synchrotron and IC (Klein-Nishina effects included) emission over a period of 1,000 - 100,000 years. This age range is appropriate for most of the identified galactic plane TeV sources which are significantly extended. Many such sources are thought to be associated with the nebulae surrounding Vela-like pulsars, which have characteristic spin-down ages of order 10 kyr. More evolved sources are possible as well, although at least in the leptonic scenario, cooling of VHE electrons limits lifetimes to $\sim$100 kyr as we shall discuss later. Injection (and evolution) occurs in time steps much smaller than the assumed age. More complex injection spectra, such as dual components, provide adequate fits to the data as well, though we see little justification for such complications given the current limited data. We consider a low density environment with density $n = 1$ cm^{-3} (although densities of up to $n = 200$ cm^{-3} are possible, as discussed in section 2.1), and photon fields comprised of CMBR, far IR (3×10^{-3} eV, with density 1 eV cm^{-3}), and near IR (0.3 eV, with density 1 eV cm^{-3}), appropriate for a typical inner Galaxy environment (Porter et al. 2006).

3.1. Leptonic Gamma-Ray Emission Model

The simplest reasonable injection model is an electron power law with a high energy cutoff. We explore three source ages with this model: 1, 10, and 100 kyr. All ages yield comparable fits to the VHE data, though source parameters must be varied. Enhanced cooling for older sources requires a greater value for the total energy and high energy cutoff, as well as a lower magnetic field to allow high energy electrons to survive and IC upscatter to TeV energies. For a 10 kyr source one can match the data with a total injection energy of $5 \times 10^{47}\, d_3^2$ erg, an electron power law of slope -1.8, and an high energy exponential cutoff at 14 TeV. The high energy cutoff is required to push the X-ray flux below the new XMM limit; 14 TeV is the minimum allowed high energy cutoff which still matches the H.E.S.S. data. One could fit the H.E.S.S. data with a cutoff energy slightly greater than 14 TeV (this would better match the highest energy H.E.S.S. points, while worsening the match to the lower energy H.E.S.S. points), though this would require a lower magnetic field due to the X-ray constraint on synchrotron radiation. For a 14 TeV cutoff the radio and X-ray limits impose an already rather stringent upper limit on the magnetic field of 4 μG for this spectral shape. A spectral index softer than -1.8 is precluded by the radio upper limits. Such a hard

injection spectrum would be remarkable, as a slope of -1.8 is not required for any other galactic VHE source. For this electron spectrum, the synchrotron component peaks in the UV, and IC emission peaks around 1 TeV. Klein-Nishina effects suppress near IR scattering at the highest energies, so only far IR and CMB photons contribute in the VHE regime, with far IR the dominant component. Figure 4 shows the SED in this scenario, as well as the SED for ages of 1 and 100 kyr. For a source age of 1 kyr and the same power law index we require a cutoff at 8 TeV, an energy of $5 \times 10^{47}\, d_3^2$ erg, and a maximum magnetic field of 4 μG. At this young age, the radio upper limits prove far more constraining than the X-ray limits. A more aged source, at 100 kyr, has a total energy of $6 \times 10^{47}\, d_3^2$ erg, and requires a cutoff at 45 TeV and a very low magnetic field of 2 μG in order for energetic electrons to survive the synchrotron and IC cooling process.

We also explore the consequences of implementing a low energy cutoff in the injection spectrum. As discussed in section 1, a low energy cutoff is expected for a PWN paradigm; in the case of the Crab Nebula, (Kennel & Coroniti 1984) suggest a minimum injection energy of ~ 1 TeV at the wind termination shock, while (Wang et al. 2006) infer a minimum low-energy cutoff of 5 GeV for G 359.95−0.04. We inject an electron power law of slope -2, and a low energy cutoff of 10 GeV. This low energy cutoff allows the softer electron spectrum to remain consistent with the radio limits. For an age of 10 kyr, we require an exponential cutoff at 16 TeV, and a maximum magnetic field of 5 μG. Matching the VHE data requires a total of $6 \times 10^{47}\, d_3^2$ erg in electrons. Such a value is reasonable for a PWN origin; one of the best studied galactic broadband sources, the Vela X nebula surrounding the Vela pulsar, is estimated to possess $\sim 10^{48}$ erg in the form of leptons (de Jager 2007). A 1 kyr aged source requires an exponential cutoff at 12 TeV, magnetic field of 5 μG, and energy of $6 \times 10^{47}\, d_3^2$ erg. Finally, a 100 kyr aged source requires an exponential cutoff at 60 TeV, magnetic field of 2 μG, and energy of $8 \times 10^{47}\, d_3^2$ erg.

3.2. Hadronic gamma-ray emission model

A hadronic scenario relaxes the strictures imposed by the XMM upper limit, and instead one finds the radio upper limits more constraining. A proton power law with index -2 and cutoff at 50 TeV provides an adequate fit to the H.E.S.S. data, requiring energy $E = 8 \times 10^{50}\, (n/1\,\mathrm{cm}^{-3})\, d_3^2$ erg. The timescale for pion production via p-p interactions of $\tau_{pp} \approx 1.5 \times 10^8\, (n/1\,\mathrm{cm}^{-3})^{-1}$ years (Blumenthal 1970) is significantly greater than the expected age of the system, so the proton spectrum is treated as static. For this proton spectrum, we calculate the photons from proton-proton interactions and subsequent π^0 and η-meson decay following (Kelner et al. 2006). Proton-proton interactions also yield $\pi^{\pm}$ mesons which decay

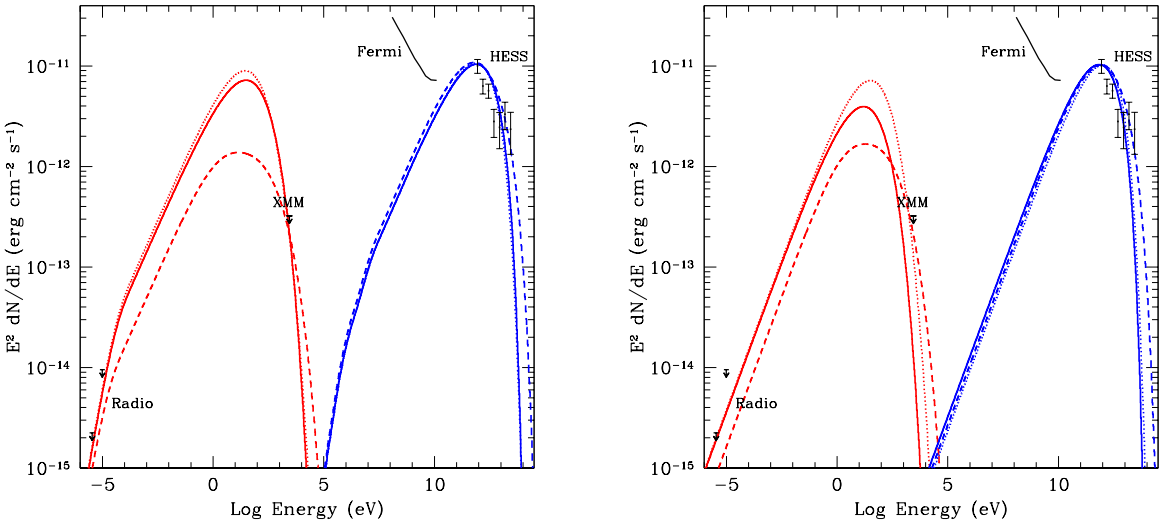

Fig. 4.— SED for leptonic scenario showing the synchrotron and total IC emission for three source ages: Left: index of -2 and low energy cutoff of 10 GeV. Solid denotes 1 kyr age (12 TeV cutoff, $B = 5\,\mu$G), dotted is 10 kyr (16 TeV cutoff, $B = 5\,\mu$G), and dashed is 100 kyr (60 TeV cutoff, $B = 2\,\mu$G). Right: index of -1.8 and no low energy cutoff. Solid denotes 1 kyr age (8 TeV cutoff, $B = 4\,\mu$G), dotted is 10 kyr (14 TeV cutoff, $B = 4\,\mu$G), and dashed is 100 kyr (45 TeV cutoff, $B = 2\,\mu$G).

into secondary electrons, which we evolve in a 5 μG field. The secondary electron spectrum is a function of the age of the system, so we evolve over 1, 10, and 100 kyr, as shown in Figure 5. IC and synchrotron fluxes from the resultant secondary electron spectrum are subsequently calculated, indicating that secondary IC is unimportant, while for high source ages one must take care to ensure the synchrotron component does not exceed the radio upper limits. We observe the π^0 gamma-rays as a broad peak in the GeV to TeV range, indicating that a Fermi detection would not be surprising.

4. Discussion

4.1. Leptonic Scenario

The steep ($\Gamma = -2.5$) H.E.S.S. TeV spectral index could imply that electrons responsible for this emission are cooled. As already discussed, in a leptonic scenario a high magnetic field is precluded (given the low TeV to X-ray flux ratio), which leaves a large age as the remaining cooling possibility. Indeed, for a source age of 1 kyr cooling is negligible, while at 10 kyr

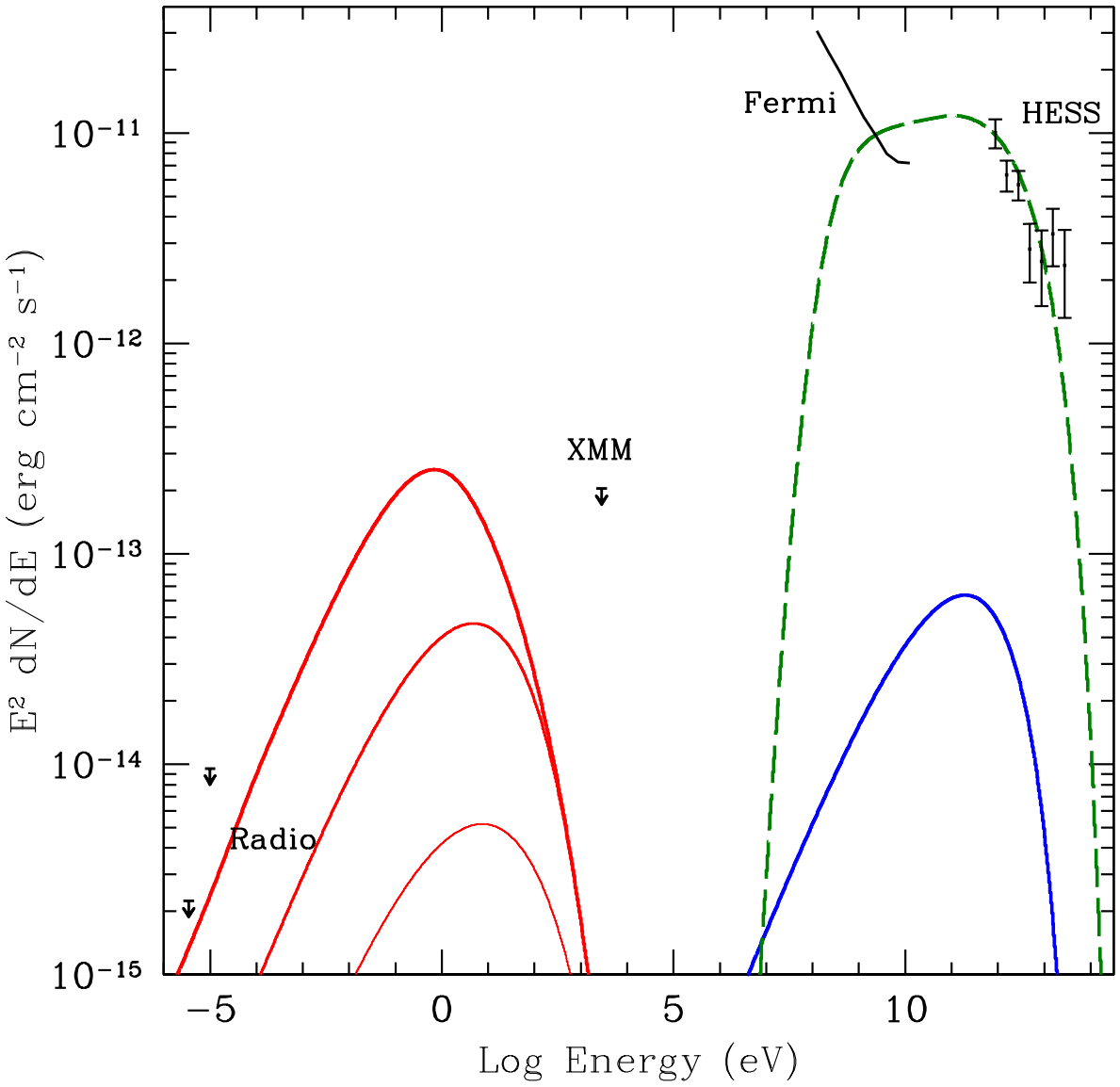

Fig. 5.— SED for a hadronic scenario: $n = 1$ cm^{-3}, $B = 5\mu$G, cutoff = 50 TeV. Solid low energy lines indicate synchrotron emission for 1, 10, 100 kyr (bolder is older), higher energy solid line is IC emission for 10 kyr. The dashed line denotes gamma-rays from pion decay. A higher ambient particle density would decrease the energy requirement in the form of hadrons, and correspondingly reduce the synchrotron and IC flux.

cooling is just beginning to affect the electrons responsible for upscattering photons to the

VHE regime (which necessitates the slightly greater value for the high energy cutoff). The mean electron energy required to IC scatter the CMB seed photons to TeV energies ($E_{\rm TeV}$) is $E_e = (18{\rm TeV})E_{\rm TeV}^{1/2}$, so the presence of gamma-rays up to 50 TeV indicates electrons must be accelerated to ~ 100 TeV levels. For more modest 10 TeV electrons, the cooling timescale for electrons IC scattering off the CMBR is $\tau_{IC} = 100\,(E/10\,{\rm TeV})^{-1}$ kyr. In regions of very low magnetic field the IC timescale is comparable to the synchrotron cooling lifetime $\tau_{sync} = 90\,(E/10\,{\rm TeV})^{-1}(B/3\,\mu{\rm G})^{-2}$ kyr. Regardless of whether electrons lose their energy primarily through IC or synchrotron, based solely on cooling timescales one might estimate J1708 to be as old as 100 kyr for very low ambient magnetic fields. One can compare this age with estimates of the diffusion timescale. A source subtending 0.07° has radius $R = 3.7 d_3$ pc. Then for a cooling limited electron source with Bohm diffusion $t_{diff} = 19\,d_3^2\,(B/3\,\mu{\rm G})(E/10\,{\rm TeV})^{-1}$ kyr. This indicates a problem; it becomes difficult to confine the VHE electrons required to power the H.E.S.S. source long enough for a cooling break to develop. This argues against a source age as high as 100 kyr, since for the canonical electron power law index of -2 we found above that significant numbers of electrons must persist up to 60 TeV to combat the high degree of cooling over such a lengthy period.

Another possibility to explain the steep H.E.S.S. spectrum is that there is a cutoff in the electron spectrum not far above the H.E.S.S. range (at some tens of TeV) corresponding to either a maximum in the acceleration energy or the escape of the highest energy electrons. A truncated accelerator provides a simple explanation, but even if the accelerator persists up to the PeV range, 100 TeV electrons tend to escape in 2 kyr or faster for Bohm diffusion. The SED fits indicate that a source aged 10 kyr will suffer some cooling due to the low magnetic field required by the X-ray limit, but the location of the IC peak still depends critically on the value of the high energy cutoff. A cut-off, rather than fully cooled, distribution of electrons therefore seems the most natural explanation for the H.E.S.S. data in the leptonic scenario, justifying our assumed injection spectrum of a power law with an exponential cutoff. Such a cutoff also argues against an age of 100 kyr, noted above.

For an age of 10 kyr one class of potential counterparts, SNRs, could easily occupy the volume assumed for a 3 kpc distance, since this implies a very reasonable mean expansion velocity of $360\,d_3\,(\theta/0.07^\circ)\,(T/10\,{\rm kyr})^{-1}\,{\rm km\,s^{-1}}$. Middle aged pulsars and their corresponding wind nebulae offer another possibility. The reverse shock from the parent SNR is expected to reach the PWN in ~ 7 kyr (Reynolds & Chevalier 1984), which (as in the case of the Vela PWN (Blondin et al. 2001)) can displace the PWN far from the parent pulsar where the magnetic field can be quite low and the the scenarios described above remain plausible. Another possibility stems from the high transverse velocity of pulsars, which typically cross their parent SNR shells after ~ 40 kyr (Gaensler & Slane 2006). At this late stage the pulsar has often escaped its original wind bubble, leaving behind a relic PWN (van der Swaluw

et al. 2004). In this environment a lack of X-ray emission is not surprising, as the ambient magnetic field can be very low, while VHE photons arise from IC scattering of the relic electrons.

4.2. Hadronic Scenario

In the hadronic scenario the high energy cutoff at 50 TeV most likely stems from either the maximum accelerator energy or the diffusive escape of the highest energy particles. The Bohm diffusion timescale predicts a loss of 50 TeV particles in ≈ 6 kyr in a 5 μG field. The assumed source age of 10 kyr would therefore be reasonable. The new XMM limit places few constraints on the model. In the radio regime, however, the flux scales as the number of electrons $n_e \times B^{3/2}$, or since we assume constant injection of particles, flux scales as the age of the system $T \times B^{3/2}$; for J1708 we find $(B/10\,\mu\mathrm{G})^{3/2}\,(T/50\,\mathrm{kyr}) < 1$. Though this limit is not very constraining, it does indicate that our assumptions for age and magnetic field are reasonable. The energy requirement of $E = 8 \times 10^{50}\,(n/1\,\mathrm{cm}^{-3})\,d_3^2$ erg is consistent with a supernova origin for ambient densities of $\sim 10\,\mathrm{cm}^{-3}$.

5. Conclusions

Independent of any model, the VHE luminosity of $L \approx 9 \times 10^{33}\,d_3^2\,\mathrm{erg\,s}^{-1}$ indicates that J1708 is a prodigious gamma-ray emitter. For comparison, the Vela X nebula surrounding the Vela pulsar is observed to have gamma-ray luminosity of only $L_{0.6-65\,\mathrm{TeV}} \approx 10^{33}\,\mathrm{erg\,s}^{-1}$ (Aharonian et al. 2006b). This would imply a high gamma-ray luminosity if J1708 originates from a PWN. We compare to the Vela PWN rather than the standard candle of VHE astronomy, the Crab, since the lack of X-rays and hence low magnetic field implies an older PWN than 1 kyr. The leptonic scenario requires fine-tuning of low and high energy cutoffs and magnetic field to match the observed H.E.S.S. flux and lower energy upper limits. While hadronic injection requires less manipulation of injection spectrum and source properties, the required energy in protons of $E_p = 8 \times 10^{50}\,(n/1\,\mathrm{cm}^{-3})\,d_3^2$ erg is quite high for low density environs. Yet if the H.E.S.S. detection stems from protons interacting with a molecular clouds of density $\sim 100\,\mathrm{cm}^{-3}$, this energy requirement is significantly relaxed. Regardless of injection species the diffusion and cooling timescales for VHE particles hint at an age of 10-50 kyr for magnetic fields in the range of $3 - 5\,\mu$G.

The currently available data do not allow us to conclusively pin down the nature of the emitting particles in J1708. A Fermi LAT detection would provide a significant boost

to understanding this source, and implies a hadron accelerator as is apparent in Figures 4 and 5. Deeper radio images would also help us to elucidate the processes at work in J1708. Further lowering the radio upper limit would constrain the spectral index of the source, and/or the low energy cutoff for leptons; for hadrons the product of age and $B^{3/2}$ would be constrained. J1708 is particularly interesting among unidentified TeV sources as it has no lower energy candidate counterparts whatsoever and is rather compact. These features, combined with its high gamma-ray luminosity, could point to a very different type of VHE system than those we currently know.

We thank NASA for supporting this research with grant NNX06AH66G.

Facilities: XMM-Newton

REFERENCES

Abdo, A. A., et al. 2009, ApJS, 183, 46

Aharonian, F., et al. 2006, Nature, 439, 695

Aharonian, F., et al. 2006, A&A, 448, L43

Aharonian, F., et al. 2006, ApJ, 636, 777

Aharonian, F., et al. 2007, A&A, 467, 1075

Aharonian, F., et al. 2008, A&A, 477, 353

Blondin, J. M., Chevalier, R. A., & Frierson, D. M. 2001, ApJ, 563, 806

Blumenthal, G. R. 1970, Phys. Rev. D, 1, 1596

Brand, J., & Blitz, L. 1993, A&A, 275, 67

Dame, T. M., Hartmann, D., & Thaddeus, P. 2001, ApJ, 547, 792

de Jager, O. C. 2007, ApJ, 658, 1177

Dickey, J. M., & Lockman, F. J. 1990, ARA&A, 28, 215

Duncan, A. R., Stewart, R. T., Haynes, R. F., & Jones, K. L. 1995, MNRAS, 277, 36

Gaensler, B. M., & Slane, P. O. 2006, ARA&A, 44, 17

Green, A. J., Cram, L. E., Large, M. I., & Ye, T. 1999, ApJS, 122, 207

Hinton, J. A., & Hofmann, W., 2009, Annual Reviews of Astronomy and Astrophysics (in press)

Kalberla, P. M. W., Burton, W. B., Hartmann, D., Arnal, E. M., Bajaja, E., Morras, R., Pöppel, W. G. L. 2005, A&A, 440, 775

Kelner, S. R., Aharonian, F. A., & Bugayov, V. V. 2006, Phys. Rev. D, 74, 034018

Kennel, C. F., & Coroniti, F. V. 1984, ApJ, 283, 710

Porter, T. A., Moskalenko, I. V., & Strong, A. W. 2006, ApJ, 648, L29

Reynolds, S. P., & Chevalier, R. A. 1984, ApJ, 278, 630

van der Swaluw, E., Downes, T. P., & Keegan, R. 2004, A&A, 420, 937

Wang, Q. D., Lu, F. J., & Gotthelf, E. V. 2006, MNRAS, 367, 937